

APPLICABILITY OF EMPIRICAL GREEN'S FUNCTION METHOD TO STRONG MOTION RECORDS ON MAN-MADE ISLAND IN KOBE

Atsushi NOZU¹ And Tatsuo UWABE²

SUMMARY

Empirical Green's function (EGF) method has been applied to the records at Port Island during 1995 Hyogo-ken Nanbu Earthquake and its aftershocks to evaluate the nonlinear effect on the mainshock records with special attention to two distinguished phases which are estimated to represent direct S wave and reverberating S wave inside the basin. Kamae and Irikura's [1998] source model has been adopted. The results can be summarized as follows.

1. Direct S phase during the mainshock can be successfully reproduced with EGF method by taking into account the nonlinear behavior of the local soft soil layers above GL-83m.
2. On the other hand, the second phase seems to have already lost approximately 60% of its amplitude before its incidence to Port Island due to nonlinearity. This loss of amplitude may be attributed to the non-linear soil behavior during its first reverberation on the free surface.

Nonlinear ground response analysis shows that this kind of amplitude reduction during reverberation can exist under certain condition.

INTRODUCTION

Evaluation of soil nonlinearity is important for the prediction of strong ground motion if the site is located on soft soil layers. The strong motion record obtained on a man-made island called 'Port Island' by Kobe City Government during 1995 Hyogo-ken Nanbu Earthquake is a typical example of records which are affected by soil nonlinearity including liquefaction [e.g. Aguirre and Irikura, 1997]. Another important feature of the site is that it is located on a sedimentary basin. Because of its location, some of the aftershock records include not only direct S phase but also another distinguished phase, which is estimated to represent reverberating S wave inside the sedimentary basin. In this study, empirical Green's function (EGF) method has been applied to the records to evaluate the nonlinear effect during the mainshock on both of these two distinguished phases.

DATA

The location of Port Island is indicated in Figure 1 with a solid triangle. This site is located on a sedimentary basin, whose edge is approximately 3km to the north of the site. Three components of accelerogram were obtained at four different depths, namely, GL-0m, GL-16m, GL-32 and GL-83m during the mainshock and aftershocks. Since horizontal records at GL-83m were found to deviate clockwise [e.g. Ansary et al., 1995], they were corrected by rotating 22°counterclockwise. Aftershock records at GL-16m were excluded from this study because these records showed unusual behavior. Aftershock records were band pass filtered between 0.2-2.0Hz and integrated in frequency domain to obtain ground motion velocities. Figure 2 shows ground motion velocities at GL-0m during aftershock 1, 2 and 3. Fault normal (N37°W) components and

¹ Visitor in Civil Engineering, California Institute of Technology, Pasadena, U.S.A. Email: nozu@caltech.edu

² Structural Engineering Division, Port and Harbour Research Institute, Japan Email: uwabe@cc.phri.go.jp

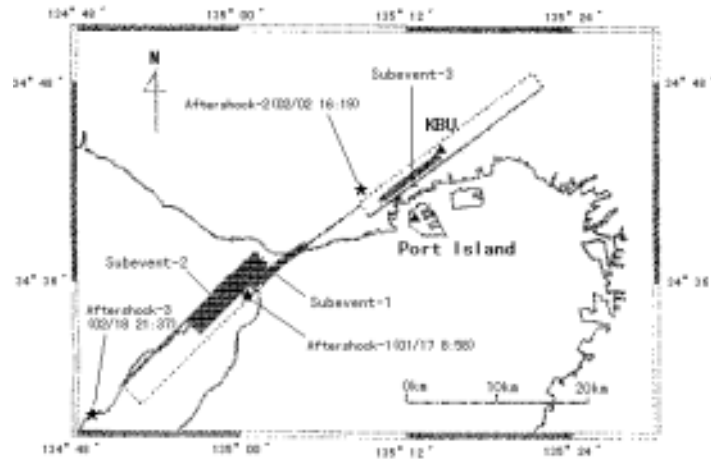


Figure 1: Location of Port Island, aftershocks and subevents of the mainshock presented by Kamae and Irikura [1998] (modified from Figure 2 in their paper)

fault parallel (N53°E) components were obtained by rotating original NS and EW components. Epicenters of the aftershocks are shown in Figure 1 with stars. Source parameters of the aftershocks are summarized in Table 1.

Table 1: Source parameters of the aftershocks

	Date	Time	Latitude (deg)	Longitude (deg)	Depth (km)	Magnitude (JMA)
Aftershock 1	1995/01/17	08:58	34.59	135.01	18.8	4.7
Aftershock 2	1995/02/02	16:19	34.70	135.15	17.9	4.2
Aftershock 3	1995/02/18	21:37	34.45	134.81	12.6	4.9

All of these records are characterized by two remarkable phases: direct S phase and another distinguished phase which is approximately 4 seconds later than direct S phase. In Figure 2, these phases are indicated as S₁ and S₂, respectively. On the other hand, Figure 3 shows ground motion velocities at Kobe University (KBU, see Figure 1) during aftershock 3. KBU is a site which has been considered more or less as a rock site. The original velocity records were band pass filtered between 0.2 and 2.0Hz. The phase S₂, which is remarkable in Port Island records, cannot be seen in KBU records. Therefore, phase S₂ seems to represent site effects. Let us restrict ourselves to the records of aftershocks 1 and 3 and examine the records relatively in detail because these records seem to be representative of subevent 1 of the mainshock [Kamae and Irikura, 1998], which controls the strong ground motion at Port Island during the mainshock. It can be observed that both S₁ and S₂ are propagating upward inside the soft soil layers. Table 2 summarizes the average phase velocities of S₁ and S₂ between accelerometers. These phase velocities are obtained by reading the difference of the locations of peaks in the original accelerograms. Phase velocities for aftershock 1 is smaller because it occurred only three hours after the main shock and the effect of nonlinear behavior during the mainshock was still remaining. Phase velocities of S₁ and S₂ are

Table 2: Average phase velocities of S1 and S2 (m/s)

	aftershock 1		Aftershock 3	
	S1	S2	S1	S2
(GL-32m)-(GL-0m)	139	139	152	152
(GL-83m)-(GL-32m)	319	319	364	340

practically identical if we consider the fact that Δt is 0.01s for these records. Therefore, we can safely say that phase S₂ was propagating vertically as an S wave at least within the soft soil layers in Port Island. It is likely, therefore, that phase S₂ represents reverberating S wave within the basin. This idea is supported by the S-wave velocity structure model of the Osaka sedimentary basin [Kagawa et al., 1998], in which two way travel time of S wave is 3.2s. Although the time lag of S₁ and S₂ are larger than 3.2s, this discrepancy may be explained if we assume that the ray of s₂ was not necessarily vertical as shown schematically in Figure 4. Large amplitude of S₂ may be attributed to focusing effects. Another interesting feature of the records of aftershocks 1 and 3 is that,

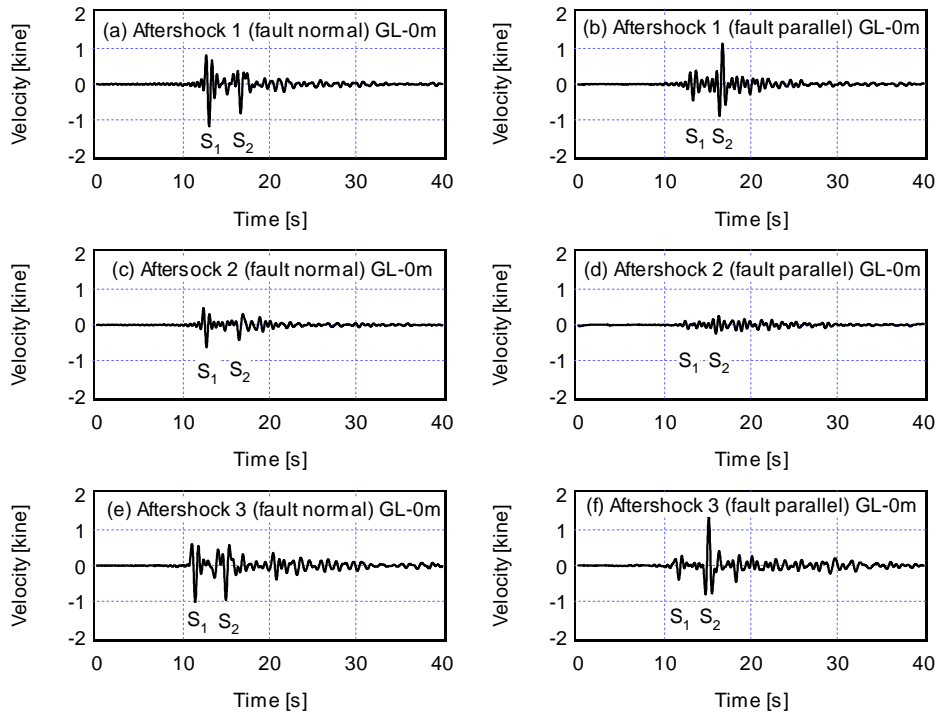


Figure 2: Ground motion velocities at Port Island GL-0m during aftershock 1 (top), aftershock 2 (middle) and aftershock 3 (bottom)

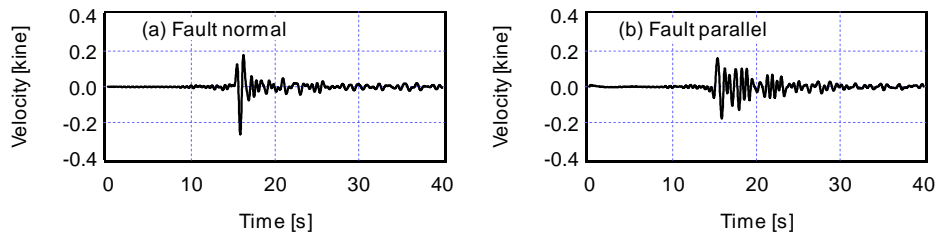


Figure 3: Ground motion velocities at Kobe University (KBU) during aftershock 3

although the predominant direction of direct S wave (S_1) is perpendicular to the fault as expected from the theory, fault-parallel component is larger for the second phase (S_2). This fact indicates that the second phase is affected by the existence of horizontal heterogeneity of the media, that is, the basin edge. All of these facts lead to the estimation of the propagation path of S_1 and S_2 as illustrated in Figure 4. The direction of particle motion is allowed to rotate clockwise at the moment of incidence of S_2 into the sedimentary basin in this model. In the following sections, it is assumed that the second distinguished phase in the aftershock records represents reverberating S wave within the sedimentary basin.

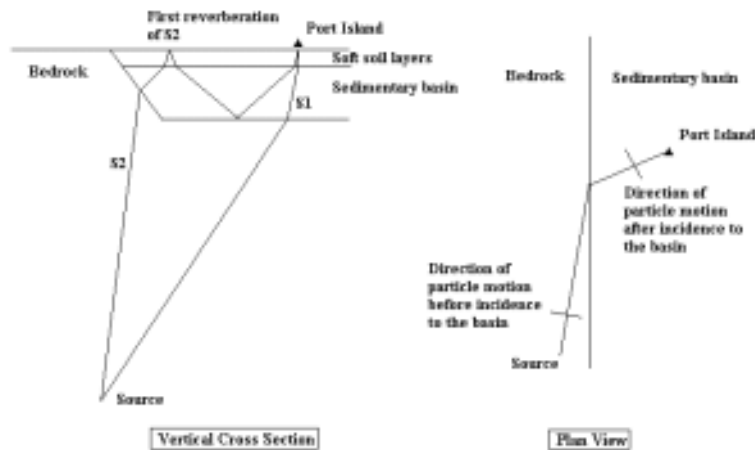


Figure 4: Schematic diagram of estimated rays for S_1 and S_2

METHOD

Empirical Green's Function (EGF) Method [Irikura, 1983] was used in this study. We made it sure that the method gives practically the same results as his revised method [Irikura, 1986] in our case as long as low frequency (0.2-2.0Hz) velocity waveforms are concerned. The superposition can be expressed as follows.

Here, $U(t)$ and $u(t)$ denote ground motions during the large and small events, respectively. r , r_{ij} and r_0 denote the

$$U(t) = C \sum_{i=1}^N \sum_{j=1}^N \sum_{k=1}^N \frac{r}{r_{ij}} u(t - t_{ij} - (k-1) \frac{\tau_r}{N}) \quad (1)$$

$$t_{ij} = \frac{r_{ij} - r_0}{\beta} + \frac{\xi_{ij}}{V_R} \quad (2)$$

distance from the site to the hypocenter of the small event, to the (i,j) element of the large event and to the rupture starting point of the large event, respectively. ξ_{ij} is the distance from the rupture starting point to the (i,j) element of the large event, β is the shear wave velocity, V_R is the rupture velocity and τ_r is the rise time of the large event. N is the scaling parameter and C is the stress drop ratio for the large and small events.

Kamae and Irikura's [1998] source model was adopted for the synthesis of the ground motion during the large event. This source model consists of three subevents as shown in Figure 1. Aftershock 3 was selected to represent subevents 1 and 2 and aftershock 2 was selected to represent subevent 3 to assure that the same propagation path is shared between the ground motion from the small event and the subevent of the large event. The record of aftershock 1 was not used because it is affected by the nonlinear soil behavior during the main shock. Parameters in Table 3 were used so that the ground motion at KBU during the mainshock can be successfully reproduced. This reproduction is shown in Figure 5.

Table 3: Green's function and parameters for each subevent

	Green's function	N	C
Subevent 1	Aftershock 3	6	1.9
Subevent 2	Aftershock 3	10	1.0
Subevent 3	Aftershock 2	10	1.0

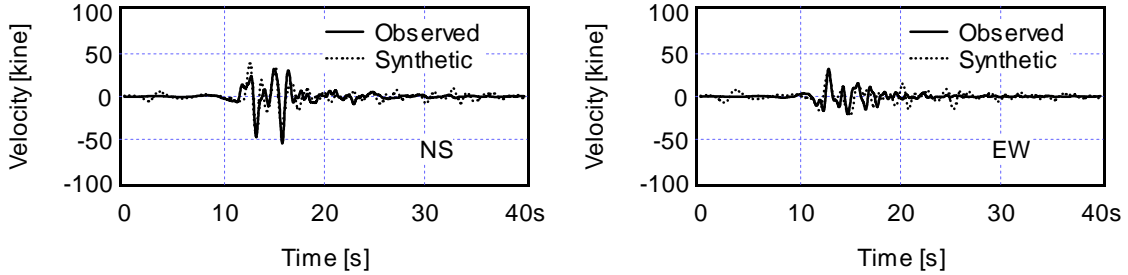


Figure 5: Comparison between observed motions at KBU and synthetics with parameters given in Table 3 (Both observed motions and synthetics were band pass filtered between 0.2-2.0Hz)

NONLINEAR BEHAVIOR OF LOCAL SOFT SOIL LAYERS

In Figure 6, observed ground velocities at Port Island (band pass filtered between 0.1-2.0Hz and integrated in frequency domain from original accelerograms) are compared with synthetic ground motions which are obtained assuming linear behavior of the whole media. Aftershock records at GL-0m were used to obtain synthetics at GL-0m and then it was used to obtain synthetics at other depths by using linear theory. Obviously the results overestimate the ground motions because the actual soil behavior during the mainshock was nonlinear.

To take into account the soil nonlinearity, EGF method was combined with nonlinear effective stress analysis of the soil. First, the synthetics at the free surface was deconvolved to obtain incident waveforms at GL-83m assuming linear soil behavior. Then this incident wave was used as an input motion for the non-linear effective stress analysis of the soil. This analysis was performed with FLIP [Iai et al., 1992]. The effect of liquefaction is considered in this analysis. The model parameters for the analysis were determined by referring to the results of geotechnical investigations. For the purpose of demonstrating the validity of the model parameters, the observed

ground motion at GL-83m was used as an input motion to compute ground motions at other depths. As shown in Figure 7, the results show good agreement with the observations, indicating the validity of the soil parameters.

The results of the combination of EGF method and FLIP are shown in Figure 8. As shown in Figure 8, the direct S phase (S_1) during the mainshock is successfully reproduced with this method. It should be noted that the incident waveform at GL-83m is assumed not to be affected by soil nonlinearity in this method. The success of the reproduction of the direct S phase indicate that the direct S phase had not been affected by soil nonlinearity until it's incidence to the local soft soil layers of Port Island.

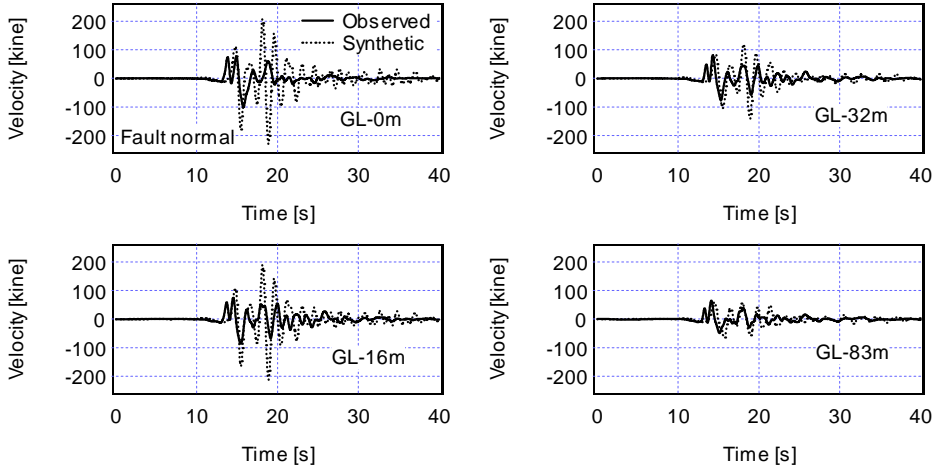


Figure 6: Comparison of observed ground velocities and synthetics with linear theory

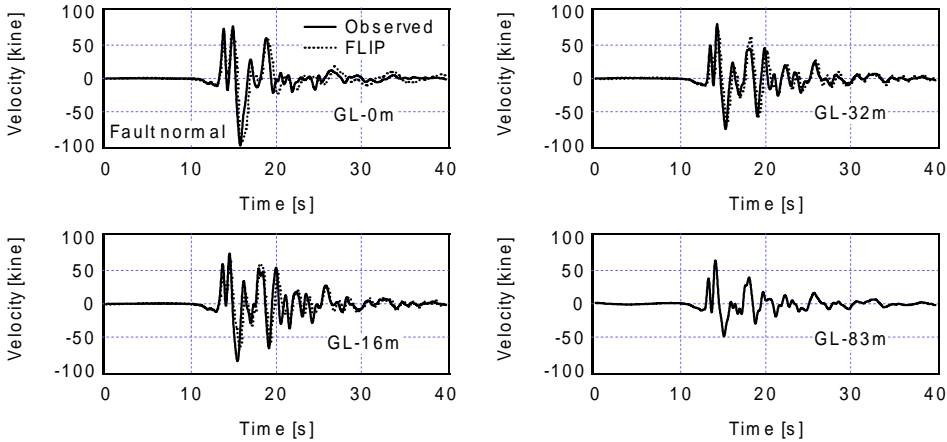


Figure 7: Comparison of observed ground velocities with the results of nonlinear effective stress analysis (FLIP) in which observed ground motion at GL-83m was used as an input motion

NONLINEAR SOIL BEHAVIOR DURING FIRST REVERBERATION OF S_2

Although the direct S phase (S_1) was successfully reproduced in the above analysis, discrepancy is found in the amplitude of the second distinguished phase (S_2), especially for the ground motion at GL-83m. It is likely that the second phase had been already affected by soil nonlinearity before it's incidence to the local soft soil layers. As shown in Figure 9, the second phase during the mainshock is successfully reproduced with EGF method if we assume that it had lost approximately 60% of it's amplitude before it's incidence to Port Island. This loss of amplitude may be attributed to the non-linear soil behavior during it's first reverberation on the free surface.

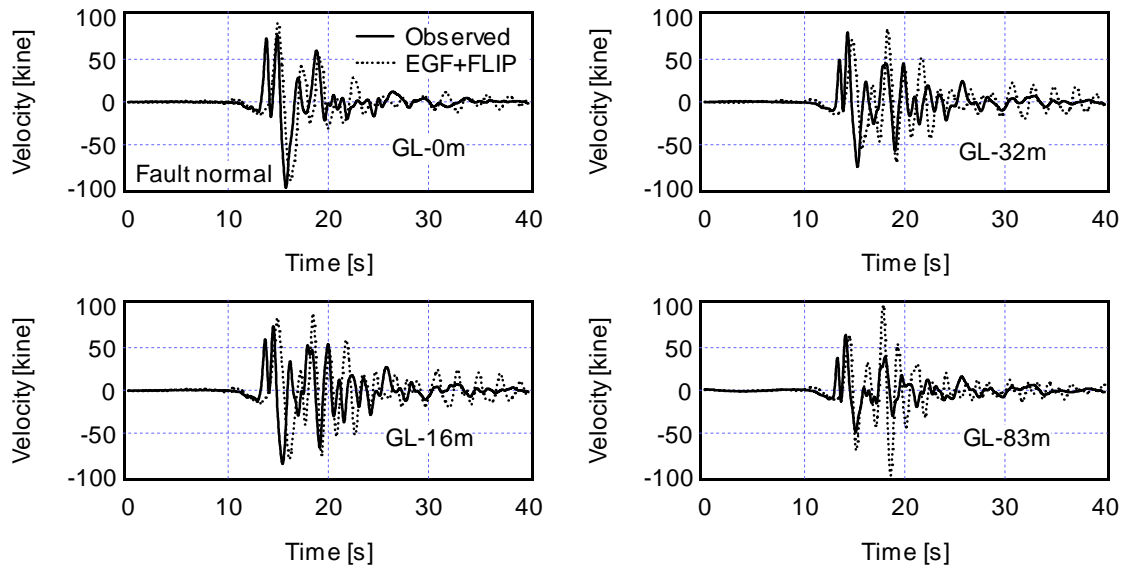


Figure 8: Comparison of observed ground velocities and synthetics in which nonlinearity of the local soft soil layers is considered with FLIP

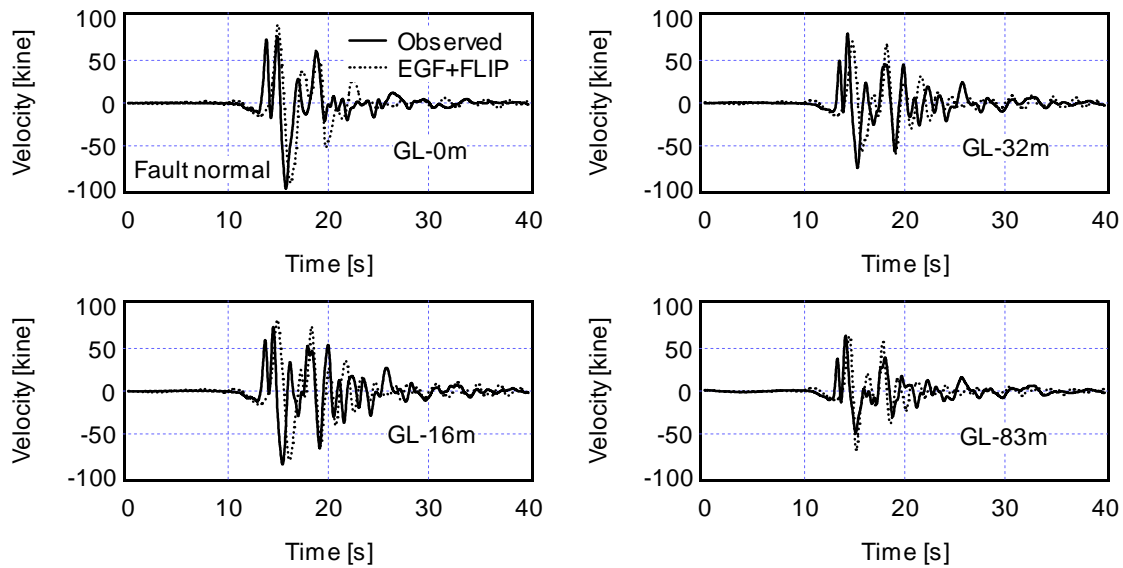


Figure 9: Comparison of observed ground velocities and synthetics in which nonlinearity of the local soft soil layers is considered with FLIP. Besides, the second phase is assumed to have lost 60% of its amplitude before its incidence to the local soft soil layers.

It is difficult to simulate this process accurately with nonlinear analysis because we cannot specify the location of the first reverberation of S_2 . Here, nonlinear effective stress analysis was performed for the same soil layers as Port Island just to demonstrate that this kind of amplitude reduction during reverberation can exist under certain condition. Time derivative of Ricker wavelet with peak velocity of 50kine was used as the incident waveform (see Figure 10). As shown in Figure 10, the amplitude of reflected wave is approximately 60% smaller than expected from linear theory in this case.

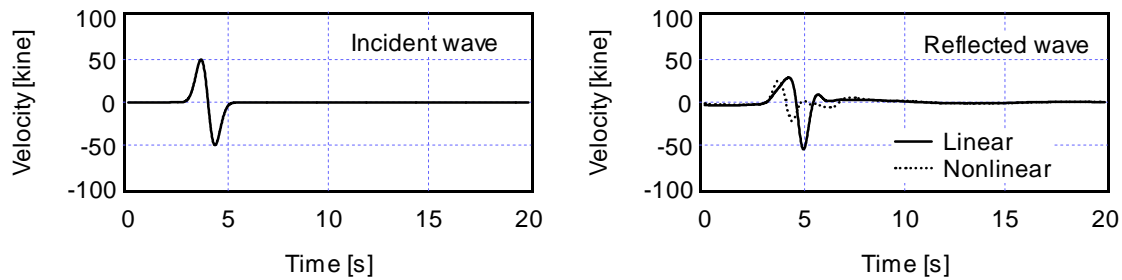


Figure 10: Assumed incident wave (left) and computed reflected waves (right) for the nonlinear effective stress analysis which was performed for the purpose of demonstrating the amplitude reduction during reverberation due to nonlinearity

CONCLUSIONS

1. Direct S phase during the mainshock can be successfully reproduced with EGF method by taking into account the nonlinear behavior of the local soft soil layers above GL-83m.
2. On the other hand, the second phase seems to have lost approximately 60% of its amplitude before its incidence to Port Island due to nonlinearity. This loss of amplitude may be attributed to the non-linear soil behavior during its first reverberation on the free surface.
3. Nonlinear ground response analysis shows that this kind of amplitude reduction during reverberation can exist under certain condition.

ACKNOWLEDGMENTS

We thank Dr. Sumio Sawada at Disaster Prevention Research Institute, Kyoto University for his helpful suggestions. Downhole array records at Port Island were kindly provided by Kobe City Government. Records at Kobe University were recorded by the Committee of Earthquake Observation and Research in the Kansai Area (CEORKA).

REFERENCES

- Aguirre, J. and Irikura, K. (1997), "Nonlinearity, Liquefaction, and Velocity Variation of Soft Soil Layers in Port Island, Kobe, during the Hyogo-ken Nanbu Earthquake", *Bulletin of the Seismological Society of America*, Vol.87, No.5, pp.1244-1258.
- Ansary, M. A., Yamazaki, F., Katayama, T and Towhata, I.(1995), "Analysis of Ground Motions at Liquefied Site during the 1995 Great Hanshin Earthquake", *23rd Earthquake Engineering Workshop*, JSCE, pp.277-280.
- Iai, S., Matsunaga, Y. and Kameoka, T. (1992), "Strain Space Plasticity Model for Cyclic Mobility ", *Soils and Foundations*, Vol.32, No.2, pp.1-15.
- Irikura, K. (1983), "Semi-Empirical Estimation of Strong Ground Motions during Large Earthquakes ", *Bulletin of Disaster Prevention Research Institute, Kyoto University*, Vol.32, pp.63-104.
- Irikura, K. (1986), "Prediction of Strong Acceleration Motion Using Empirical Green's Function", *Proceedings of the 7th Japan Earthquake Engineering Symposium*, pp.151-156.
- Kamae, K. and irikura, K.(1998), "Source Model of the 1995 Hyogo-ken Nanbu Earthquake and Simulation of Near-Source Ground Motion", *Bulletin of the Seismological Society of America*, Vol.88, No.2, pp.400-412.
- Kagawa, T., Sawada, S, Iwasaki, Y and Nanjo, A.(1998), "S-Wave Velocity Structure Model of the Osaka Sedimentary Basin Derived from Microtremor Array Observations", *Zisin 2*, Vol.51, No.1, pp.31-40 (in Japanese).